Rate Constant and Mechanism of the Reaction of OH Radicals with Acetic Acid in the Temperature Range of 229−300 K

N. I. Butkovskaya,* A. Kukui,† N. Pouvesle, and G. Le Bras

CNRS, Laboratoire de Combustion et Systèmes Réactifs, 1C Av. de la Recherche Scientifique, 45071 Orléans Cedex 2, France, and CNRS, Service d'Aéronomie, Paris, France

Received: April 8, 2004; In Final Form: June 4, 2004

The overall rate constant for the reaction OH + CH_3COOH → products in the temperature range of 229−300 K was determined using a chemical ionization mass spectrometer coupled to a high-pressure turbulent flow reactor (∼200 Torr of carrier gas N_2). A strong negative temperature dependence of the rate constant was found in this range which can be expressed in Arrhenius form as $k_1(T) = ((2.2 \pm 0.2) \times 10^{-14}) \exp((1012 \pm 80)/T)$ cm^3 molecule^{-1} s^{-1} with $k_1 = 6.6 \times 10^{-13}$ cm^3 molecule^{-1} s^{-1} at 298 K. When these results are combined with previous measurements in the range of 298−446 K,[8] a three-parameter expression can be derived: $k_1(T) = (2.45 \times 10^{-16})(T/298)^{5.24\pm0.68} \exp((2358 \pm 189)/T)$ cm^3 molecule^{-1} s^{-1}, describing the curvature of the Arrhenius plot observed at $T > 300$ K. A branching fraction of (64 ± 17)% was determined between 300 and 249 K for the H-atom abstraction from the carboxyl group OH + CH_3COOH → CH_3 + CO_2 + H_2O. This latter parameter was measured as the yield of CO_2, formed as a result of the fast decomposition of the primary $CH_3C(O)O$ radical. Atmospheric implications of the obtained results are discussed. The obtained k_1 value provides a lifetime of CH_3COOH in the upper troposphere (UT) that is a factor of 2 lower than that calculated so far from existing recommendations. The data also show that acetic acid could be as significant as methane in influencing the oxidative capacity of the UT considering that concentrations of CH_3COOH from hundreds of pptv to a few ppbv have been measured during several campaigns.

Introduction

Oxygenated volatile organic compounds (VOCs) are significant trace species in the atmosphere which have important implications for the atmospheric HO_x budget. Among these compounds, acetic acid has been recently recognized as potentially important. Acetic acid is photochemically produced in the troposphere, mainly from reactions of the peroxy acetyl radicals $CH_3C(O)OO$ with peroxy radicals HO_2 and CH_3O_2.[1] A global photochemical source strength of 120 Tg/year was reported by Baboukas et al.[2] Direct emissions of CH_3COOH are evaluated as 48 Tg/year originating mainly from biomass burning.[3] Though a large part of the emitted acetic acid is dissolved in water and washed out from the low troposphere, it can be directly transported to high altitudes by continental outflows, and a mixing ratio of CH_3COOH up to 2 ppbv has been measured in the tropical upper troposphere.[4] Such high concentrations suggest that acetic acid could be a source of methyl peroxy radicals as important as methane in the upper troposphere (UT).[4] However, atmospheric sources and sinks of acetic acid are not yet well-known, and acetic acid concentrations are not well reproduced in most models.[5]

The major loss process of CH_3COOH in the UT is considered to be its gas-phase reaction with OH radicals:

$$OH + CH_3COOH \rightarrow \text{products} \qquad (1)$$

Only a few studies have been dedicated to this reaction.[6−8] The temperature dependence of the overall rate constant of reaction 1 was investigated in two flash photolysis/resonance spectroscopy studies in the range of 298−446 K, giving contradictory results.[7,8] Dagaut et al.[7] obtained a slight increase of the rate constant from 298 to 440 K, whereas Singleton et al. observed a significant decrease with increase of temperature from 298 to 446 K. The existing recommendations are based on the average of these data and give a slight negative temperature dependence $k_1 = (4 \times 10^{-13}) \exp(200 \pm 400/T)$ cm^3 molecule^{-1} s^{-1} with $k_1 = 8.0 \times 10^{-13}$ cm^3 molecule^{-1} s^{-1} at 298 K.[9,10] The recommended value at 298 K is somewhat higher than (6.0 ± 0.8) × 10^{-13} cm^3 molecule^{-1} s^{-1} reported in the earlier study of Zetzsch and Stuhl.[6]

The reaction can proceed by two hydrogen atom abstraction channels:

$$OH + CH_3COOH \rightarrow CH_3 + CO_2 + H_2O \qquad (1a)$$

$$\rightarrow CH_2COOH + H_2O \qquad (1b)$$

Though the products of reaction 1 were not investigated, channel 1a is expected to be the preferential pathway despite the fact that the C−H bond dissociation energy in the methyl group of CH_3COOH is several kcal mol^{-1} lower than in the carboxyl group: $D_0(H-CH_2COOH) \approx 98$ kcal mol^{-1} and $D_0(CH_3C(O)O-H) \approx 106$ kcal mol^{-1}.[8] This expectation is based on the measurements of the primary kinetic isotope effect (KIE) in CD_3COOH and CD_3COOD reactions carried out by Singleton et al.[8] The lack of a primary KIE for OH + CD_3COOH and a large decrease in reactivity observed upon D-substitution on the carboxylic site led to the conclusion that the preferential pathway is the H-atom abstraction from the carboxyl group (pathway 1a).

* Corresponding author. Permanent address: Institute of Chemical Physics of the Russian Academy of Sciences, 117334 Moscow, Russian Federation.

† Service d'Aéronomie.

10.1021/jp048444v CCC: $27.50
Published on Web 08/04/2004

In the present work the overall rate constant of the OH + CH_3COOH reaction was measured in the temperature range of 229−300 K using a turbulent flow reactor connected to a chemical ionization mass spectrometer. The decay of OH radical at different concentrations of CH_3COOH was monitored by detecting OH^- ions. Acetic acid concentration was measured on-line using absorption spectroscopy. Dimerization of acetic acid was taken into account in the evaluation of its concentrations in the reactor. The branching fraction of the abstraction of carboxylic hydrogen was determined in the 248−300 K range by the measurement of the CO_2 yield with detection of CO_2 as CO_3^- ion.

Experimental Section

The high-pressure turbulent flow reactor (HPTFR) coupled with a chemical ionization mass spectrometer (CIMS) used in the present study has been previously described.[11] The reactor was a Pyrex tube of 2.4 cm inner diameter. The pressure in the reactor was 200 Torr, and the flow velocity of the N_2 carrier gas was about 18 m/s. Before entering the reactor, the N_2 passed through a glass reservoir with molecular sieves. The mixing and flow conditions were determined by the Reynolds number Re = 6300, which ensured a plug flow and a turbulent mixing of the reactants. The validation tests of the flow conditions have already been reported.[11] The cooling of the reactor was achieved by flowing the N_2 carrier gas through a trap with molecular sieves located in a Dewar vessel filled with liquid nitrogen. The required temperature was maintained using a CB100 digital controller providing PID automatic regulation of the heating of the inlet main flow tube connecting the cool trap with the reactor. A Pt100 resistance temperature detector inserted in the middle of the reactor served as a temperature input of the controller. Two K-type thermocouples were used to measure the temperature at both ends of the reactor.

A movable injector of 1.1 cm inner diameter served as a prereactor to produce OH radicals in the reaction

$$F + H_2O \rightarrow OH + HF \qquad (2)$$

F-atoms were generated by microwave discharge in F_2/He gas mixtures in a quartz tube of 0.6 cm inner diameter concentrically connected with the injector. The concentration of H_2O in the injector was about 1×10^{14} molecule cm^{-3}, which was sufficient to totally consume the F-atoms during the residence time in the injector. The drawback of this source is the formation of oxygen atoms during the discharge in fluorine. However, reaction 2 was preferred to reaction 3 in order to obviate reactions of OH radicals with NO_2 and NO. The maximal distance from the injector tip to the orifice of the inlet cone of the mass spectrometer was 55 cm, which corresponded to a reaction time in the HPTFR of about $t_r \approx 32$ ms. The OH radical signal was calibrated by measuring consumption of NO_2 in an excess of H-atoms using the reaction

$$H + NO_2 \rightarrow OH + NO \qquad (3)$$

During the calibration, NO_2 was introduced into the main reactor and H_2/He mixture into the discharge tube. Typical concentrations of OH in the reactor during the kinetic measurements were $(2 \div 6) \times 10^{11}$ molecule cm^{-3}. Tank grade H_2 and F_2 (Alpha Gas 2) were used without further purification. NO_2 was purified by keeping its mixture with O_2 for 24 h followed by pumping out the oxygen through a liquid N_2 trap. After that, NO_2 diluted in He (∼1%) was stored in a glass flask.

Acetic acid (Fluka, glacial 99.9%) was introduced into the reactor upstream of the tip of the movable injector along with the He flow passing through a trap containing the liquid acid. The sample was additionally purified in thaw-and-pump cycles with the selection of the middle fraction. The acetic acid concentration in the reactor was varied in the range of $(7 \div 80) \times 10^{12}$ molecule cm^{-3}. The acid concentration was measured on-line by optical absorption. The CH_3COOH/He flow passed through an absorption cell with a 1 m optical length crossed by a beam emitted from a Zn lamp and detected at $\lambda = 213.8$ nm. The absorption cross sections at this wavelength for the monomer and the dimer of acetic acid are $\sigma_M = (1.35 \pm 0.20) \times 10^{-19}$ and $\sigma_D = (1.84 \pm 0.37) \times 10^{-19}$ cm^2 $molecule^{-1}$.[12] Accordingly, the observed absorption corresponds to the sum

$$\ln(I_0/I) = L\,(\sigma_M\,[M] + \sigma_D\,[D]) \qquad (E1)$$

where I_0 is the reference light beam intensity, I is the intensity of the beam in the presence of acid, and L is the optical path length. The concentrations of the monomer, [M], and the dimer, [D], are related via the equilibrium constant[13]

$$K_{eq}\,(atm^{-1}) = [D]/[M]^2 = (2.80 \times 10^{-8}) \exp(7290/T) \qquad (E2)$$

The above equations with $T = T_{cell}$ allow the determination of the monomer and dimer concentrations in the optical cell. As the absorption is weak, concentrations of the order of 10^{15} molecule cm^{-3} were needed in the cell for reliable spectroscopic measurements. The cell was heated to $T = 330$ K to at least partly destroy the CH_3COOH dimers. We avoided heating at higher temperature because of the possible change of the absorption cross sections.[12] The number of acetic acid molecules can be calculated as [M] + 2[D], which directly corresponds to the concentration in the reactor when the amount of dimer in the reactor is insignificant, as, for example, at room temperature. At lower temperatures, the monomer concentration in the reactor was calculated using equation E2 with $T = T_{reactor}$. In most of the measurements the concentration of the dimer was negligible. It exceeded 10% of the monomer concentration in only a few experiments below 250 K. The rate constant of the reaction of OH with the dimer was directly measured in the work of Singleton et al.[8] and found to be $k_D = 9.2 \times 10^{-15}$ cm^3 $molecule^{-1}$ s^{-1} (with an upper limit of 3.5×10^{-14} cm^3 $molecule^{-1}$ s^{-1}) at 297 K. It supposedly decreases with the decrease of temperature, making the role of the dimer in our measurements of no importance. Uncertainties in the CH_3COOH concentrations arise mainly from the errors in the absorbance, temperature (which defines the equilibrium), and dimerization equilibrium constant. In addition to the quoted uncertainties for the absorption cross sections, the error in the absorbance includes the inaccuracy of the light detector, about 2%. The temperature in the absorption cell was measured with ±0.2°C accuracy. The uncertainties of the temperature in the reactor were as follows: 300 ± 0.2, 269 ± 1, 247 ± 2, and 229 ± 4 K. The $K_{eq}(T)$ expression was taken from the most recent reports.[13] Comparing with the $K_{eq}(T)$ values used in refs 7, 8, and 12 and on the basis of earlier thermodynamical data from ref 14, we estimated the uncertainty as $\ln K_{eq} = -(17.36 \pm 0.13) + (7290 \pm 144)/T$. Accordingly, the accuracy of the measured CH_3COOH concentrations varied with temperature and was estimated to be 17% at 300 K. For lower temperatures, the CH_3COOH concentration uncertainties are indicated in Table 1.

The ion−molecular reactor (IMR) was a stainless steel tube of 4 cm inner diameter and 40 cm length connected with the chemical reactor and the quadrupole analyzer (EXTREL) by

TABLE 1: Rate Constant for the OH Reaction with CH_3COOH at Various Temperatures[a]

T (K)	$[CH_3COOH]$	$[(CH_3COOH)_2]$	$k_1[CH_3COOH]$	k_1[b]
300	0.92 ± 0.15		5.5	6.6 ± 0.3 (± 1.1)
	1.91 ± 0.32		11.2	
	2.96 ± 0.50		18.8	
	3.95 ± 0.67		26.8	
	4.98 ± 0.84		32.6	
	8.12 ± 1.54		52.5	
269	0.59 ± 0.10		7.1	8.9 ± 0.5 (± 1.6)
	1.31 ± 0.22	0.01	13.3	
	2.24 ± 0.38	0.03	21.8	
	3.70 ± 0.63	0.09	37.0	
	4.91 ± 0.84	0.15	43.3	
253[c]	0.53 ± 0.16	0.01	8.1	11.2 ± 2.1 (± 2.3)
	1.16 ± 0.44	0.05	11.4	
	2.12 ± 0.76	0.18	25.0	
251	1.09 ± 0.20	0.02	11.0	13.6 ± 3.2 (± 4.2)
	1.80 ± 0.32	0.07	29.7	
	3.68 ± 0.66	0.25	48.6	
247	0.89 ± 0.16	0.05	13.0	13.1 ± 2.5 (± 3.5)
	2.47 ± 0.44	0.37	33.9	
	3.49 ± 0.76	0.80	45.7	
229	0.52 ± 0.09	0.16	8.0	18.3 ± 3.7 (± 5.0)
	0.79 ± 0.14	0.38	14.7	

[a] Concentrations are in units of 10^{13} molecule cm^{-3}; bimolecular rate constants are in units of 10^{-13} cm^3 $molecule^{-1}$ s^{-1}. [b] k_1 error limits near the value are two standard deviations in the slopes in Figure 2; error limits in parentheses are the total uncertainties. [c] Measured with the $H + NO_2$ reaction as a source of OH radicals.

nozzles of 1 and 0.3 mm diameter, respectively.[11] The flow velocity of Ar carrier gas in the IMR was about 20 m s^{-1} at 0.7 Torr. Ar was purified by passing it through a liquid N_2 trap. The primary Ar^+ ions and free electrons were generated in the ion source using a heated filament. A flow of SF_6 was continuously introduced into the IMR downstream of the ion source. The primary SF_6^- negative ions were produced by attachment of thermalized electrons to SF_6. Hydroxyl radicals and NO_2 (for calibration) were detected as OH^- (*m*/*e* 17) and NO_2^- (*m*/*e* 46) ions formed by electron transfer from SF_6^-. CO_2 molecules were detected as CO_3^- ions (*m*/*e* 60) using the ion−molecular reaction[15]

$$O_3^- + CO_2 \rightarrow CO_3^- + O_2 \quad (4)$$

In turn, O_3^- ions were produced by adding a small quantity of ozone to the SF_6 flow:[16]

$$SF_6^- + O_3 \rightarrow O_3^- + SF_6 \quad (5)$$

The CIMS signal representing CO_2 was linear in the range of $(1 \div 50) \times 10^{11}$ molecule cm^{-3}. Unfortunately, the CO_3^- ions in the present study interfered with the d_1 natural isotopic peak of the $CH_3CO_2^-$ ion from the mass spectrum of acetic acid:

$$SF_6^- + CDH_2COOH\ (CH_3COOD) \rightarrow CDH_2CO_2^- + HF + SF_5 \quad (6)$$

Overlapping of the peaks increased the noise level at *m*/*e* 60 which significantly reduced the accuracy of the CO_2 yield measurements.

Results and Discussion

Rate Constant of the OH + CH_3COOH Reaction. The decay of OH radicals at different concentrations of CH_3COOH was measured at $T = 300$, around 265, around 250, and 229 K.

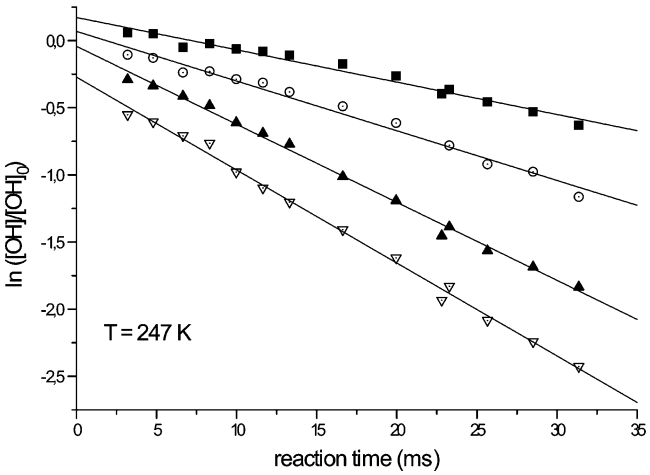

Figure 1. Decay of OH radical concentrations at 247 K. Concentrations in the reactor (in molecule cm^{-3}): $[OH] = 4 \times 10^{11}$; $[CH_3COOH] = 8.9 \times 10^{12}$ (⊙); 2.5×10^{13} (▲); 3.5×10^{13} (▽); absence of acetic acid (■).

The study of the reaction

$$OH + CH_3COOH \rightarrow \text{products} \quad (1)$$

was conducted under pseudo-first-order conditions in a large excess of CH_3COOH over OH. Figure 1 presents an example of the measured decay time profiles for $T = 247$ K. The first-order rate constants were calculated as the difference of the slopes in the presence and in the absence of acetic acid in the reactor. It was found that the decay of OH radicals in the absence of acetic acid always followed first-order kinetics with a rate constant of about 20 s^{-1}. It did not depend on the OH concentration and was practically independent of the temperature in the reactor. This loss could not be explained by self-reaction and was attributed to unknown reactions of OH with the products of the discharge or wall loss. Some data (for 253 K) were acquired using the reaction $H + NO_2$ (reaction 3) as a source of OH radicals. During these measurements, NO_2 was introduced through the injector so that its concentration in the reactor was 2.2×10^{12} molecule cm^{-3}. This led to an increased decay of OH due to the $OH + NO_2$ addition reaction, which rate was 25 s^{-1} in the absence of acetic acid, while the calculated reaction rate was $k_3[NO_2] = 12$ s^{-1} with $k_3 = 5.3 \times 10^{-12}$ cm^3 $molecule^{-1}$ s^{-1} at $P = 200$ Torr of N_2.[9] The noticeable difference between the observed decay and the loss in the reaction with NO_2 indicates that walls could play some role in the OH kinetics. Table 1 contains the determined $k_1[CH_3COOH]$ values for all the temperatures. The dependence of the obtained first-order rate constants on the acetic acid concentration is shown in Figure 2. It has to be noted again that in most of the measurements the concentration of the dimer was insignificant, except at $T = 229$ K, when the concentration of the dimer in the reactor represented 31% and 48% of that of the monomer for the two acid concentrations presented in Figure 2, and further increase of CH_3COOH flow resulted in a domination of the dimer in the reactor. For comparison, dimer fractions at the highest acid concentrations used at 247, 269, and 300 K were 23%, 3.1%, and 0.2%, respectively (see Table 1).

The Arrhenius plot of the derived rate constants for reaction 1 is shown in Figure 3 by solid triangles. These data can be expressed in Arrhenius form as $k_1(T) = ((2.2 \pm 0.2) \times 10^{-14}) \exp((1012 \pm 80)/T)$ cm^3 $molecule^{-1}$ s^{-1}, which formally corresponds to a negative activation energy of about 2 kcal mol^{-1} (solid line). The room-temperature value, $k_1(298) = 6.6$

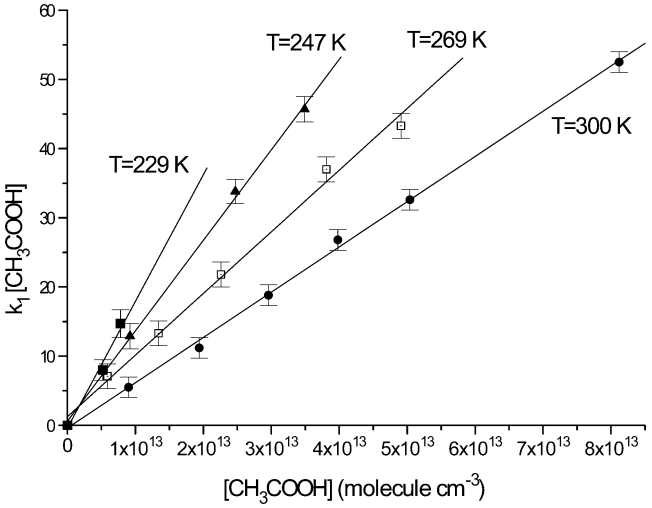

Figure 2. Plot of the pseudo-first-order rate constant against acetic acid concentration at different temperatures.

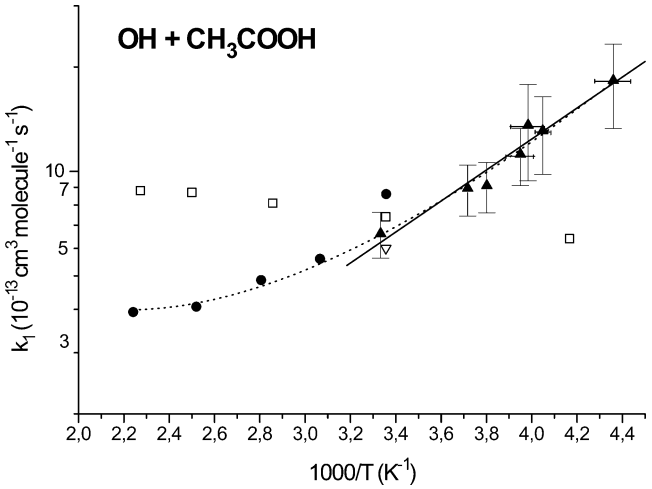

Figure 3. Arrhenius plot for k_1. Results of the present work (▲) are compared with existing literature data from Dagaut et al.[7] (□), Singleton et al.[8] (●), and Zetzsch and Stuhl[6] (▽) (see text for discussion).

$\times$ 10^{-13} cm^3 molecule^{-1} s^{-1}, falls between the rate constant values obtained by Zetzsch and Stuhl, $(6.0 \pm 0.8) \times 10^{-13}$ cm^3 molecule^{-1} s^{-1},[6] and Dagaut et al., $(7.4 \pm 0.6) \times 10^{-13}$ cm^3 molecule^{-1} s^{-1},[7] the value of Singleton et al., $k_1(298) = (8.6 \pm 0.6) \times 10^{-13}$ cm^3 molecule^{-1} s^{-1},[8] being slightly higher. The temperature change of k_1 we observed is in agreement with the results of Singleton et al.[8] When our data are combined with their results for the 326−446 K range, a three-parameter expression can be derived, $k_1(T) = (2.45 \times 10^{-16}) (T/298)^{5.24\pm0.68} \exp((2358 \pm 189)/T)$ cm^3 molecule^{-1} s^{-1}, describing the curvature observed at $T > 298$ K (dashed curve in Figure 3).

There is a discrepancy of our results with the rate constant of Dagaut et al. at 240 K,[7] and there is also a disagreement between the results of Dagaut et al. and Singleton et al.[8] giving different temperature dependences of the rate constant. The latter has been already discussed in the work of Singleton et al.,[8] where the possible errors in the determination of the CH_3COOH concentration in the study of Dagaut et al.[7] were indicated. In particular, the low rate constant obtained at 240 K originates from the assumption of equal reactivity of the individual acid groups in the dimer and the monomer, i.e., that the dimer reacts 2 times faster than the monomer. Accordingly, their rate constant at 240 K was "normalized for the CH_3COOH unit concentration", i.e., [M] + 2[D]. The authors do not give the exact conditions but state that the major species in the reactor cell

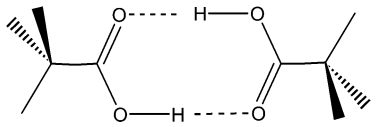

Figure 4. Structure of the acetic acid dimer.

were the dimers. Evidently, if their reported rate constant is multiplied by a factor of ([M] + 2[D])/[M], it would be in better agreement with our measurements.

The observed negative temperature dependence can be explained by a formation of the prereactive hydrogen-bonded complex of the H-atom of the hydroxyl with the oxygen end of carboxyl group of the acid. Furthermore, recent calculations of the potential energy surface (PES) of the OH + CH_3COOH reaction at high levels of theory up to G2M//B3LYP-DFT/6-311++G(2df,2pd) showed that the H-bond remains intact in the H-abstraction transition state, both for abstraction of the methyl and acidic hydrogen.[17] This feature of the PES qualitatively explains the higher propensity for abstraction of the acidic hydrogen. It is important that the reaction with the methyl H-atoms also proceeds via the addition−elimination mechanism. This mechanism can also explain the low reactivity of the CH_3-COOH dimers toward the OH radicals. The acidic hydrogens are bonded with the oxygen atoms of the other molecule as schematically shown in Figure 4. This hydrogen bonding does not allow abstraction of the bonded H-atoms and, which is very important, prevents formation of the complex with OH so that only the direct abstraction from the methyl groups is available. Direct abstraction of the primary hydrogen atoms is a relatively slow process and, moreover, strongly decreases with the decrease of temperature. This was demonstrated experimentally in the work of Singleton et al.,[8] where the rate constants for the reaction of OH radicals with the acetic acid dimer $k_D = 9.2 \times 10^{-15}$ and 1.1×10^{-13} cm^3 molecule^{-1} s^{-1} were obtained at 297 K and at 326 K, respectively.

Branching Ratio for the OH + CH_3COOH Reaction: Determination of the Yield of CO_2. The branching fraction of channel 1a was determined as the ratio of the produced concentration of CO_2 molecules to the consumed concentration of OH radicals in reaction 1:

$$k_{1a}/k_1 = \Phi(CO_2) = \Delta[CO_2]/\Delta[OH]_{Ac} \qquad \text{(E3)}$$

The CO_2 concentration produced was measured at $t_r = 30$ ms. The signal of CO_2 was calibrated using the pre-prepared 3% mixture of CO_2 in He. The mixture was introduced into the reactor maintaining the H_2O, F_2, and CH_3COOH flow rates the same as during the measurement of the CO_2 signal from the reaction. The concentration of CO_2 was calculated from the measured pressure drop in a calibrated volume. $\Delta[OH]_{Ac}$ was determined from the OH signal measured at the minimal reaction time of 2.4 ms, $[OH]_0$, and at $t_r = 30$ ms in the absence ($[OH]_f$) and in the presence ($[OH]_{fa}$) of CH_3COOH:

$$\Delta[OH]_{Ac} = ([OH]_0 - [OH]_{fa}) \ln([OH]_{fa}/[OH]_f)/\ln([OH]_{fa}/[OH]_0) \qquad \text{(E4)}$$

This expression is a solution of the system of the two first-order kinetic equations describing OH decay in the absence (E5) and in the presence (E6) of acetic acid

$$[OH]_f = [OH]_0 \exp(-k_0 t_r) \qquad \text{(E5)}$$

$$[OH]_{fa} = [OH]_0 \exp(-k_0 t_r - k' t_r) \qquad \text{(E6)}$$

TABLE 2: CO_2 Yield from the OH Reaction with CH_3COOH[a]

T (K)	$[CH_3COOH]$	$[OH]_0$[b]	$\Delta[OH]$[c]	$\Delta[OH]_{Ac}$[d]	I_{60}[e]	$\Delta[CO_2]$	$\Phi((CO_2)$ (%)
298	441	0.64	0.27	0.24	2665 ± 413	0.158	66 ± 15
273	404	0.44	0.31	0.20	2851 ± 642	0.123	63 ± 17
249	300	0.41	0.31	0.14	1879 ± 383	0.090	62 ± 18

[a] Concentrations are in units of 10^{12} molecule cm^{-3}. [b] Initial OH concentration. [c] Total OH consumed. [d] OH reacted with acetic acid. [e] CO_2 signal intensity in counts per second.

where k_0 is the rate constant of OH loss in the reactor without CH_3COOH, and $k' = k_1[CH_3COOH]$ is the first-order rate constant of reaction 1. From these equations we can obtain the ratio of the rate constants expressed in terms of the OH initial and final concentrations

$$k'/(k_0 + k') = \ln([OH]_{fa}/[OH]_f)/\ln([OH]_{fa}/[OH]_0) \quad \text{(E7)}$$

The hydroxyl radicals consumed by CH_3COOH can be determined by the integration

$$\Delta[OH]_{Ac} = \int k'[OH]_0 \exp(-k_0 t - k_1 t)\, dt = [OH]_0\{k'/(k_0 + k')\}(1 - [OH]_{fa}/[OH]_0)$$

which after the substitution of E7 gives E4.

The concentrations of the reactants and the CO_2 yield obtained are given in Table 2. A slight increase of the branching factor for reaction 1a with temperature is observed, but it does not exceed the experimental error limits. The average yield, $\Phi(CO_2) = (64 \pm 17)\%$, indicates that channel 1a is the major one over the whole temperature range of 249−298 K. This result confirms the indirect observation of Singleton et al.[8] and the theoretical calculation of Vereecken and Peeters.[17] Both the branching ratio value and the observed temperature trend for the rate constant of reaction 1 are very similar to that observed by Vaghjiani and Ravishankara for the $OH + CH_3OOH$ reaction:[18]

$$OH + CH_3OOH \rightarrow CH_3O_2 + H_2O \quad \text{(7a)}$$

$$\rightarrow CH_2OOH + H_2O \quad \text{(7b)}$$

They observed a two-channel mechanism with a slight negative temperature dependence for both measured rate constants k_7 and k_{7a}, giving $k_{7a}/k_7 = 0.70$ at 298 K and $k_{7a}/k_7 = 0.67$ at 244 K. In both reactions 1 and 7 abstraction from the methyl group is significant and must be accounted for in simulation schemes. It is also interesting to compare the specific rate constant for the abstraction from the carboxylic group in reaction 1 at 298 K, $k_{1a} = 4.2 \times 10^{-13}$ cm^3 $molecule^{-1}$ s^{-1}, with the rate constant of the reactions of OH radicals with perfluorinated acids, $F(CF_2)_nCOOH$ ($n = 1-4$) very recently studied at 296 K by Hurley et al.[19]

$$OH + CF_3COOH \rightarrow CF_3CO_2 + H_2O \quad \text{(8)}$$

$$OH + F(CF_2)_nCOOH \rightarrow \text{products}, \quad (n = 2-4) \quad \text{(9)}$$

and for which $k_8 = (9.4 \pm 2.1) \times 10^{-14}$ and $k_9 = (1.6 \pm 0.2) \times 10^{-13}$ cm^3 $molecule^{-1}$ s^{-1} were obtained. The lower reactivity compared to that of acetic acid can be caused by both the inductive effect and the decrease of the steric factor due to the larger size of fluorine atoms compared to hydrogen atoms which hinders formation of the prereactive complex.

Atmospheric Implications. Since photolysis does not contribute to the atmospheric destruction of acetic acid,[12] the measured rate constants at low temperatures allow the determination of a lifetime of acetic acid in the upper troposphere of 9.4 days ($\tau = (k_1[OH])^{-1}$ with $k_1 = 2.2 \times 10^{-12}$ cm^3 $molecule^{-1}$ s^{-1} at 220 K and $[OH] = 5.5 \times 10^5$ molecule cm^{-3}). This lifetime is more than a factor of 2 lower than has been calculated so far according to existing recommendations[9,10] in the absence of data at low temperature.

The impact of acetic acid oxidation in the UT can be compared with that of methane, since both acetic acid through channel 1a and methane produce methyl radicals in the primary oxidation step. In air, a rapid conversion to methyl peroxy radicals takes place:

$$OH + CH_3COOH\ (+O_2) \rightarrow CH_3O_2 + CO_2 + H_2O \quad \text{(1a)}$$

$$OH + CH_4\ (+O_2) \rightarrow CH_3O_2 + H_2O \quad \text{(10)}$$

The relative rate of production of CH_3O_2 calculated for the average measured mixing ratios of 2 ppb of CH_3COOH and 1700 ppb of CH_4[4] can be calculated as

$$\frac{d[CH_3O_2]_{Ac}/dt}{d[CH_3O_2]_{Me}/dt} = \frac{k_{1a}\,[CH_3COOH]\,[OH]}{k_{10}\,[CH_4]\,[OH]} = \frac{(2.2 \times 10^{-12})(0.64)(2)}{(7.5 \times 10^{-16})(1700)} \approx 2.2$$

with $k_{10}(T) = (2.46 \times 10^{-12}) \exp(-1780/T)$ cm^3 $molecule^{-1}$ s^{-1},[9] giving $k_{10}(220) = 7.5 \times 10^{-16}$ cm^3 $molecule^{-1}$ s^{-1}. Therefore, the production rate of CH_3O_2 from acetic acid and methane will be similar at the low temperatures of the UT. Under "NO_x rich" conditions, acetic acid could be a significant source of formaldehyde:

$$CH_3O_2 + NO \rightarrow CH_3O + NO_2 \quad \text{(11)}$$

$$CH_3O + O_2 \rightarrow CH_2O + HO_2 \quad \text{(12)}$$

As formaldehyde oxidation is a net source of HO_x, acetic acid, similarly to methane, could be a significant source of HO_x in the UT. The source could be even more important if we consider that channel 1b can also lead to the same products, CH_2O and HO_2, if decomposition of the oxy radical $CH_2(O)COOH$ is fast:

$$OH + CH_3COOH\ (+O_2) \rightarrow CH_2(O_2)COOH + H_2O \quad \text{(1b)}$$

$$CH_2(O_2)COOH + NO \rightarrow CH_2(O)COOH + NO_2 \quad \text{(13)}$$

$$(+O_2)\ 9\ CH_2O + CO_2 + HO_2$$

If reaction with O_2 is faster than decomposition

$$CH_2(O)COOH + O_2 \rightarrow CH(O)COOH + HO_2 \quad \text{(14)}$$

$$(+2O_2)\ 9\ 2HO_2 + CO + CO_2$$

more HO_x molecules are produced compared to reaction 13.

Under "NO_x poor" conditions, reactions 1a and 1b will lead to formation of CH_3OOH and $HOOCH_2C(O)OH$, respectively. The latter, most probably, will thermally decompose giving $HO_2 + CO_2 + CH_2O + OH$. The former can either photolyze to give in the presence of O_2 the same products, $CH_2O + HO_2 + OH$, or react with OH, producing $CH_3O_2 + H_2O$ (reaction 7a)

or $CH_2O + OH + H_2O$ (reaction 7b). The two different pathways (7a and 7b) have been previously discussed,[18] emphasizing that pathway 7a leads to chain termination, while formation of CH_2O in pathway 7b is a net HO_x source in the atmosphere.

In summary, the present data show that acetic acid could play a significant role in the oxidation capacity of the UT, comparable to methane, if acetic acid concentrations are at the high levels measured in ref 4 over the South Atlantic basin. This relative role of acetic acid versus methane is also significant at the lower but still high CH_3COOH concentrations measured in the UT over the western Pacific ocean[20] and over Europe[21] with mean values in the range of 117−630 pptv and 110−357 pptv, respectively. This would not be the case, however, considering the much lower concentrations (≈20 pptv) observed over the Atlantic ocean in the northern hemisphere.[22]

Conclusions

The present study reports the first measurement of the overall rate constant of the $OH + CH_3COOH$ reaction below 298 K. The observed negative temperature dependence of k_1 in the 229−300 K range is consistent with a mechanism where a prereactive [$OH \cdot CH_3COOH$] complex is formed as suggested by Singleton et al.[8] and supported theoretically by Vereecken et al.[17] The CIMS detection of the CO_2 product showed that hydrogen abstraction from the carboxylic group is the major pathway of reaction 1 between $T = 300$ and 248 K with a branching fraction of $(64 \pm 17)\%$.

For atmospheric application, the present data provide a lifetime of CH_3COOH in the UT that is a factor of 2 lower than that calculated from the recommended k_1 value in the absence of data at low temperature. The data also show that acetic acid could be as significant as methane in influencing the oxidative capacity of the upper troposphere if concentrations of CH_3COOH from hundreds of pptv to a few ppbv that have been measured during several campaigns are considered.

Acknowledgment. This work has been carried out within the EU UTOPIHAN-ACT project EVK2-CT2001-00099. We thank J. Sabatier and A. Quilgars for valuable technical assistance.

References and Notes

(1) Tyndall, G. S.; Cox, R. A.; Granier, C.; Lesclaux, R.; Moortgat, G. K.; Pilling, M. J.; Ravishankara, A. R.; Wallington, T. J. *J. Geophys. Res.* **2001**, *106*, 12, 157.

(2) Baboukas, E. D.; Kanakidou, M.; Mihalopoulos, N. *J. Geophys. Res.* **2000**, *105*, 14, 459.

(3) Kesselmeier, J.; Staudt, M. *J. Atmos. Chem.* **1999**, *33*, 23.

(4) Jacob, D. J.; Heikes, B. G.; Fan, S.-M.; Logan, J. A.; Mauzerall, D. L.; Bradshaw, J. D.; Singh, H. B.; Gregory, G. L.; Talbot, R. W.; Blake, D. R.; Sachse, G. W. *J. Geophys. Res.* **1996**, *101*, 24235.

(5) von Kuhlmann, R.; Lawrence, M. G.; Crutzen, P. J.; Rasch, P. J. *J. Geophys. Res.* **2003**, *108*, 4729.

(6) Zetzsch, C.; Stuhl, F. *Phys. Chem. Behav. Atmos. Pollut. Proc. Eur. Symp.* **1982**, 69.

(7) Dagaut, Ph.; Wallington, T. J.; Liu, R.; Kurylo, M. J. *Int. J. Chem. Kinet.* **1988**, *20*, 331.

(8) Singleton, D. L.; Paraskevopoulos, G.; Irwin, R. S. *J. Am. Chem. Soc.* **1989**, *111*, 5248.

(9) Sander, S. P.; Friedl, R. R.; Golden, D. M.; Kurylo, M. J.; Huie, R. E.; Orkin, V. L.; Moortgat, G. K.; Ravishankara, A. R.; Kolb, C. E.; Molina, M. J.; Finlayson-Pitts, B. J. *Chemical Kinetics and Photochemical Data for Use in Stratospheric Studies*; Evaluation No. 14; JPL Publication 02-25, Pasadena, 2003.

(10) Atkinson, R. A. *J. Phys. Chem. Ref. Data*, Suppl. 2, **1994**, 1.

(11) Kukui, A.; Borissenko, D.; Laverdet, G.; Le Bras, G. *J. Phys. Chem. A* **2003**, *107*, 5732.

(12) Orlando, J. J.; Tyndall, G. S. *J. Photochem. Photobiol. A* **2003**, *157*, 161.

(13) (a) Hasse, H.; Schmitt, M. *Vapour-Liquid Equilibria of System II*; Technical Report 2001, Programme GROWTH, Project No. GRD1 CT1999 10596, UMISAT, Manchester, 2001. (b) Gmehling, J.; Onken, U.; Arlt, W.; Grenzheuser, P.; Weidlich, U.; Kolbe, B.; Rarey, J. *Vapour-Liquid Equilibrium Data Collection*; Chemistry Data Series, Part 5: Carboxylic Acids, Anhydrides, Esters; Dechema, Frankfurt, 2002.

(14) (a) Chao, J.; Zwolinski, B. J. *J. Phys. Chem. Ref. Data*, **1978**, *7*, 363. (b) Mathews, D. M.; Sheets, R. W. *J. Chem. Soc. A* **1969**, 2203.

(15) Dotan, I.; Davidson, J. A.; Strait, G. E.; Albritton, D. L.; Fehsenfeld, F. C. *J. Chem. Phys.* **1977**, *67*, 2874.

(16) Huey, L. G.; Hanson, D. R.; Howard, C. J. *J. Phys. Chem.* **1995**, *99*, 5001.

(17) Vereecken, L.; Peeters, J. *UTOPIHAN−Act 2003 Annual Report*, 2004.

(18) Vaghjiani, G. L.; Ravishankara, A. R. *J. Phys. Chem.* **1989**, *93*, 1948.

(19) Hurley, M. D.; Sulbaek Andersen, M. P.; Wallington, T. J.; Ellis, D. A.; Martin, J. W.; Mabury, S. A. *J. Phys. Chem. A* **2004**, *108*, 615.

(20) Talbot, R. W.; Dibb, J. E.; Lefer, B. L.; Scheuer, E. M.; Bradshaw, J. D.; Sandholm, S. T.; Smyth, S.; Blake, D. R.; Blake, N. J.; Sachse, G. W.; Collins, J. E.; Gregory, G. L. *J. Geophys. Res.* **1997**, *102*, 28, 303.

(21) Reiner, T.; Möhler, O.; Arnold, F. *J. Geophys. Res.* **1999**, *104*, 13, 943.

(22) Singh, H.; Chen, Y.; Tabazadeh, A.; Fukui, Y.; Bey, I.; Yantosca, R.; Jacob, D.; Arnold, F.; Wohlfrom, K.; Atlas, E.; Flocke, F.; Blake, D.; Blake, N.; Heikes, B.; Snow, J.; Talbot, R.; Gregory, G.; Sachse, G.; Vay, S.; Kondo, Y. *J. Geophys. Res.* **2000**, *105*, 3795.